Mine Water and the Environment (2018) 37:724–733
https://doi.org/10.1007/s10230-018-0524-2

TECHNICAL ARTICLE

Permeability of the Coal Seam Floor Rock Mass in a Deep Mine Based on In-situ Water Injection Tests

Yun Wu Shuyun Zhu[1] · Tingting Zhang[1]

Received: 26 June 2017 / Accepted: 26 February 2018 / Published online: 1 March 2018

Abstract
In-situ water injection tests were carried out to study the hydraulic conductivity of the roadway floor strata in the Chengjiao coal mine. Reliable water pressure test data were obtained to assess the permeability of the floor's rock mass. The initial water pressure of the intact rock mass was greater in the first water injection test, which indicated that its permeability was low. The water pressures increased when the test was repeated, which showed that cracks had propagated in the rock mass. The maximum hydraulic conductivity of the intact rock mass was obtained from different water injection tests and the results were compared with those of the Dongtan Mine in the Yanzhou coalfield, where the floor strata is geologically similar to the Chengjiao Mine's. The test data verifies that the mine floor's intact rock mass is very water-resistant. The risk of a water inrush can be judged by the numerical relationship between this resistance and the water pressure of the limestone aquifer. These results can be useful in preventing water inrush through the floor strata in other deep mines.

Keywords Hydraulic conductivity · Roadway · Water-resistant · Water inrush

Introduction

Compared to shallow mining of coal seams, deep mining is more complicated and more prone to water inrushes (Huang et al. 2014, 2015; Liu et al. 2016). The hydraulic properties of the coal seam floor rock mass are important factors to consider when evaluating the risk of an inrush. Although many researchers have examined the risk of a water inrush based on laboratory tests, theoretical analysis, and numerical simulations, these methods cannot accurately reflect the real geological conditions of coal floor strata, because pore water pressure is different in the actual rock mass (Guo and Xu 2016; Pfunt et al. 2016), which affects its permeability. In-situ tests, such as pumping and injection tests, are commonly used to determine the permeability of rock masses (Li et al. 2014a, b; Li and Qian 2013). However, fractures and low pumping rates often make it difficult to carry out pumping tests in mining areas, so injection tests are now the preferred in-situ type tests (Jiang et al. 2014; Kitagawa and Kano 2016; Xu et al. 2012). In-situ water injection tests can truly reflect the geological conditions of a site because the flow rate of the rock mass is not limited.

The Chengjiao coal mine is located in the Yongxia mine area of the Henan province in eastern China (Fig. 1a; the black area represents Henan Province, the red point represents the mine). In this mine, seam no. 2 is stable and is an important source of coal. However, seam no. 2 is located deep underground. There are two aquifers below seam no. 2, a Carboniferous (Taiyuan formation) limestone aquifer and an Ordovician limestone (Zhu et al. 2017). According to water levels obtained from in-situ measurements at the Chengjiao Mine, the water in the Ordovician limestone has no hydraulic contact with the overlying aquifers. However, two water inrushes have occurred since mining began, with the highest inrush of 300 m^3/h. Therefore, the limestone aquifers of the Taiyuan formation have become the most significant water hazard source and threatens the safety of mining there. In addition, there is relatively little hydrogeological data for the coal seam haulage roadway, which has prevented understanding the permeability of the rock mass of the coal seam floor. In light of this, in-situ water injection tests on the rock mass of the coal seam floor were carried out in the roadway to learn its hydraulic properties, and provide a basis for evaluating the risk of an inrush from the

✉ Yun Wu Shuyun Zhu
shyzhuqiao@163.com

[1] School of Resources and Earth Science, China University of Mining and Technology, Xuzhou 221116, Jiangsu, People's Republic of China

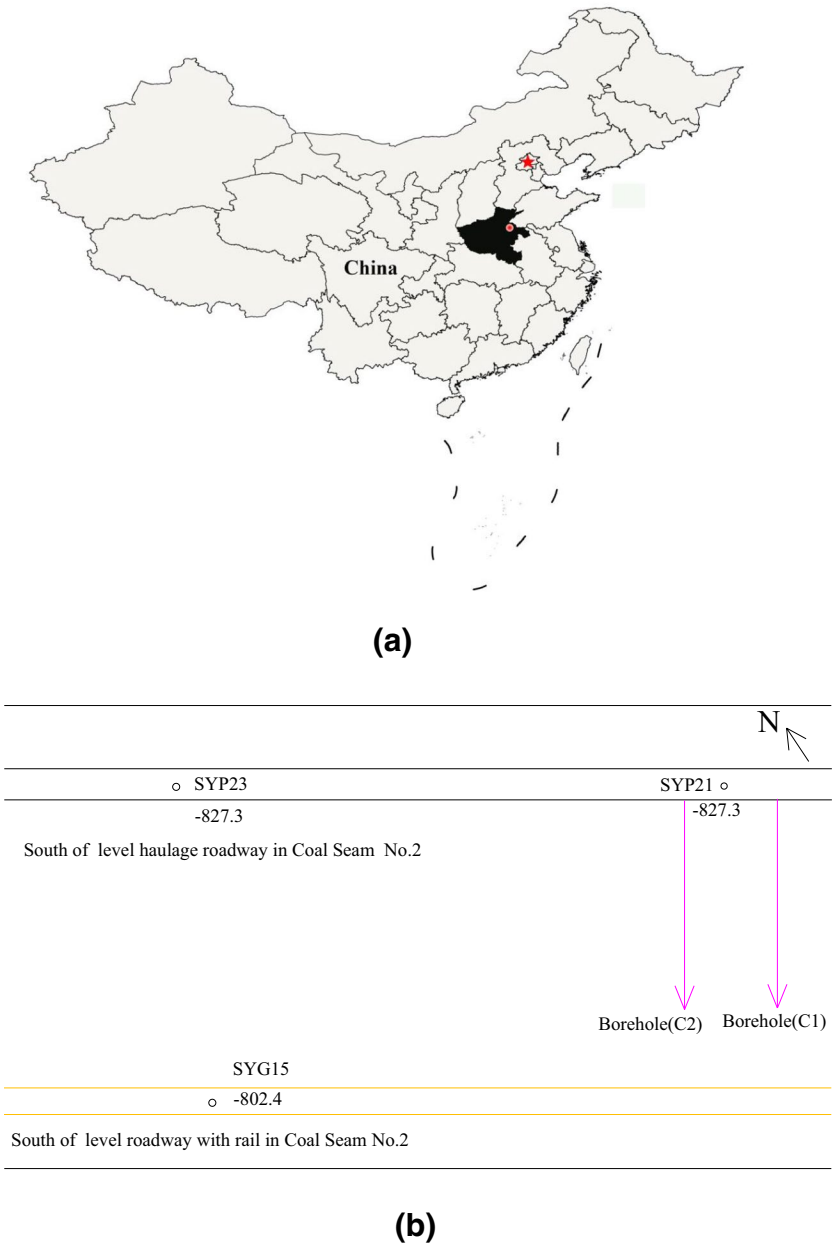

Fig. 1 Schematic of location of Chengjiao Coal Mine and layout of two boreholes

mine floor. Doing this will provide the theoretical basis for preventing and controlling inrushes through the mine floor.

Methods and Testing Equipment

Methods

The stratigraphy revealed in the coal seam no. 2 roadway was found to be relatively complete and typical. In addition, testing there would not affect normal production. Therefore, the southern portion of the roadway was chosen as the location for water injection. The control point was labeled SYP21, and test holes were drilled on both sides of SYP21. Test borehole C1 was about 2.7 m to the right of SYP21 and test borehole C2 was about 2.0 m to the left of it (Fig. 1b).

According to rock mass mechanics and theories on underground mine pressure (Jin et al. 2017; Zheng et al. 2015), there is a critical hydraulic gradient of leakage or seepage failure in the floor strata of coal seams in deep mines. Expansion of the floor strata is possible and hydraulic fractures occur when the actual hydraulic gradient exceeds the critical hydraulic gradient, thus causing water inrush from the coal seam floor due to water seepage and even failure. Two boreholes were drilled to accurately determine the permeability of the rock mass of the coal seam floor (Fig. 2).

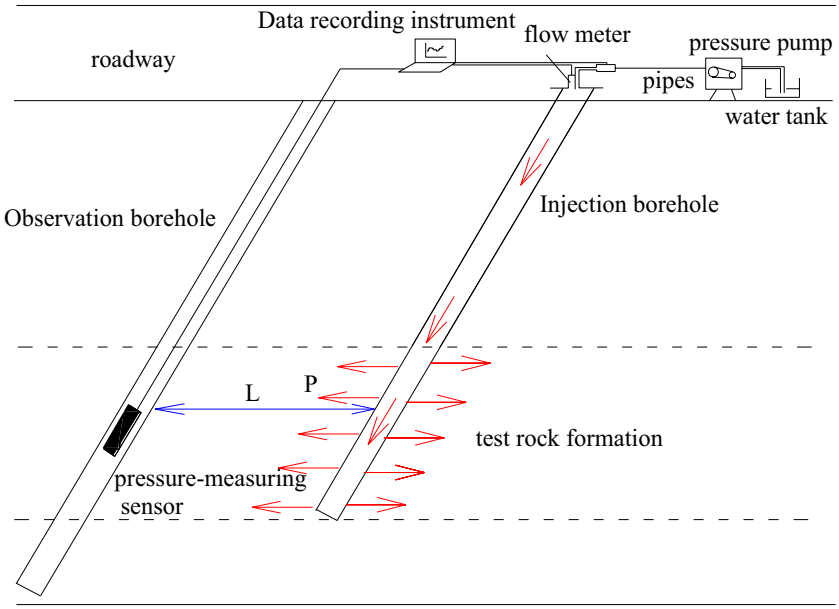

Fig. 2 Schematic of water injection test method

One of the boreholes was used for water injection and the other for observation. Casing pipes were installed and fixed by grouting, to ensure the stability of the casing pipes. A pressure measuring sensor was placed at a certain depth in the test borehole and a data recording device was installed. A flow meter, pressure pump, and the sensor were assembled together at the water injection borehole, and a GSJ-2A intelligent detector (Taian University of Science and Technology Load Cell Sensor Technology Co., LTD, China) was used to collect the data. Water pressure testing was carried out after 48 h.

Due to the lack of data on the coal seam floor strata in this mine, we examined the microstructure and water–rock characteristics of the mudstone and fine-grained sandstone by field logging and sampling. The test results showed that the rock structure and the ionic strength of the fluid are the main factors influencing the water–rock chemical interaction. Increasing the degree of micro-fracture development at the rock surface and the ionic concentration in the soaking solution increases the adsorption. This water–rock chemical interaction can damage the minerals' crystal structure, which produces microscopic fractures on the rock surface. The permeability of the coal seam floor in the depth range of the no. 2 level haulage roadway was tested and quantitative data were obtained. The strata were divided into three sections for testing within the range of the depth of the failure of the roadway, in accordance with the strata's structure. Two parallel test boreholes holes were drilled 4.7 m apart (Table 1). The lithology of the first test section is mainly fine sandstone, with an average thickness of 9.2 m. The second test section is mainly siltstone, with an average thickness of 7.2 m. The third test section is mainly sandy mudstone, with an average thickness of 20.4 m.

To conserve space, only the drilling of the test borehole in the first tested section is described in detail here:

First, boreholes C1 and C2 were drilled to a depth of 6.5 m, and casing pipes were installed and fixed by grouting. Then, C1 was drilled at a depth of 20 m, and tested at pressures of at least 6 MPa. C2 was then drilled at a depth of 32 m.

Table 1 Design parameters for drilling of two boreholes

Technical parameters	C1	C2
Diameter of opening borehole (mm)/depth (m)	150/6.5	150/6.5
Diameter of borehole (mm)	150 (0 ~ 6.5 m)–1[a] 110 (0–20.0)–3 75 (0–32.0)–8 75 (32.0–45.0)–9	150 (0–6.5 m)–4 110 (0–32.0)–6 75 (0–45.0)–11
Dip of borehole (°)	− 40	− 40
Depth of borehole (m)	45	45
Diameter of borehole casing pipe (mm)/length (m)	127/6.0–2 89/20.0–7	127/6.0–5 89/36.5–10

[a]One to eleven in the table represents order of drilling operation

After these steps were completed, a water pressure probe was installed in C2, at a controlled depth of ≈ 15 m. A pressure pump was inserted into C1 for water injection. Different injection pressures were used for each test, which each lasted for 20 min; the flow rate and water pressure in each borehole were continuously recorded. The initial water pressure was 0.5 MPa, which was gradually increased by 0.5–1.0 MPa. After applying different injection pressures, the flow rate was changed; the flow rate was first increased to the maximum rate and then reduced to 0. The water pressure probe in C2 was not removed when the tests were completed.

Testing Equipment

The primary equipment used in this study included water injection and permeability measuring devices. The water injection test was carried out using a portable, intrinsically safe, high-pressure pneumatic grout pump. The pump has gradational speed control with variable pressure, and the flow can be adjusted over a range of 5 to 80 L/min. The pumping pressure was 22 MPa, and the water pressure of the injection pipe was not less than 15 MPa. The equipment that measures the permeability included a water pressure sensor with a vibrating wire and a GSJ-2A model intelligent detector. The detector directly shows the pressure value, and can store data for later viewing. The detector is also small in size, lightweight, has a high degree of integration with other systems, and is energy efficient.

Test Results

Figure 3 shows the relationship between the water injection pressure, flow rate, and test pressure with the time of the water injection test. Since the observed water pressure was less than the water injection pressure, the former is magnified 10-fold to analyze the figure more effectively in the first test section (Fig. 3a).

Figure 3a is a plot of the water pressure of the first test section, in which the rock mass of the coal seam floor is intact. The testing time was less than 95 min. Although the water injection pressure and flow rate fluctuated, the observed water pressure increased very slowly, with an approximately linear trend, and the maximum value was only 0.10 MPa, which indicates that seepage had not started. After 95 min, the injection borehole was closed, and as the water was withdrawn, the observed and injected water pressures decreased greatly. When the first test was repeated, the observed water pressure was less than initially, and the maximum water pressure was only 0.086 MPa, but the flow rate had obviously increased. In general, the permeability of the fine sandstone is very low, and no conduction took place in either injection test.

In the second test section (Fig. 3b), with a testing time of 49 min, the water injection pressure and flow rate again tended to fluctuate; the changes in the observed water pressure basically plotted in a straight line, and the maximum value was only 0.07 MPa, which indicates that there were no seepage channels. Afterwards, the observed water pressure increased to 1.64 MPa at ≈ 60 min, which showed that seepage had started in the rock mass. Repeating the first test in this test section showed a similar variation. However, the time for any obvious increases in observed water pressure was significantly reduced, and the flow rate generally increased.

In the third test section (Fig. 3c), although the water injection pressure and flow rate tended to fluctuate in the first test, the observed water pressure increased very slowly, indicating a lack of seepage channels. The observed water pressure significantly increased after 20 min, up to 2.50 MPa, which indicates that seepage had begun in the rock mass. The observed water pressure increased more rapidly when the test was repeated, to 9.62 MPa, indicating that a large crack had likely formed in the rock mass. The flow rate also obviously increased.

Taken together, the water pressure of the three test sections demonstrated increasing stability, indicating that the permeability of the tested rock mass was low.

Discussions

Analysis of Initial Seepage Conditions

We defined the initial seepage point as the point where the water pressure in the test borehole and seepage flow obviously changed (Fig. 4). The corresponding water injection pressure of the initial seepage flow is referred to as P_{w0}. This initial pressure is the main source of the seepage in the rock mass. The seepage resistance is the ratio of the P_{w0} and the distance between the two boreholes. The parameters of the initial permeability of the three test sections of the intact rock mass of the coal seam floor can be determined by the P_{w0}, seepage pressure difference, and seepage resistance (Table 2).

The minimum value of P_{w0} is 7.50 MPa (Table 2). Although the observed water pressure is relatively low, there is still a large difference in seepage pressure. In the three test sections, the rock mass has a relatively high seepage resistance. This indicates that the permeability of the intact rock mass of the coal seam floor is low, and the seepage channels are mainly micro-cracks, which leads to greater seepage resistance.

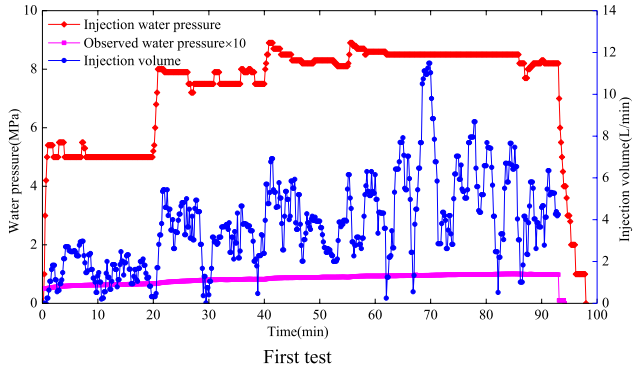

First test

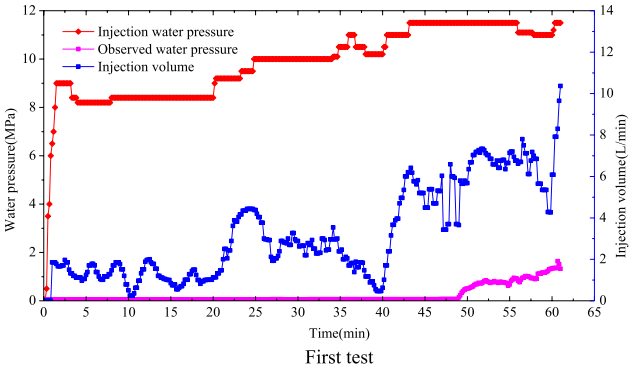

First test

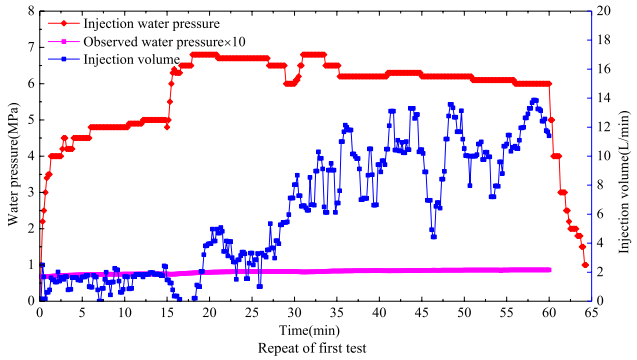

Repeat of first test

(a) First test section

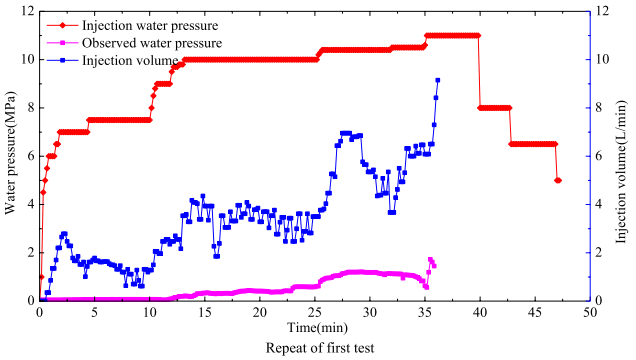

Repeat of first test

(b) Second test section

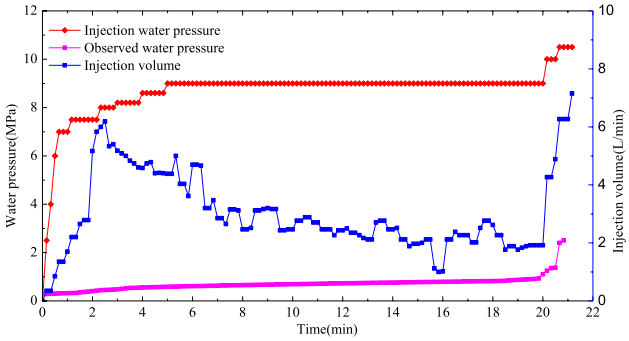

First test

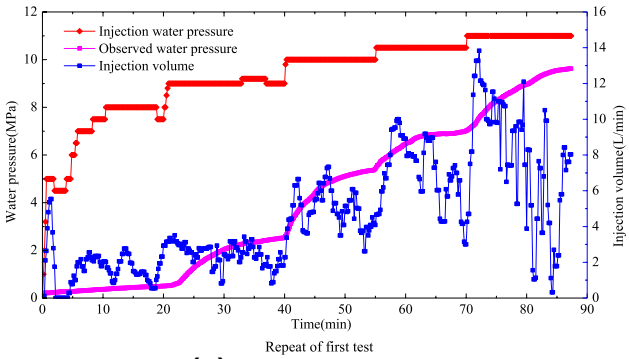

Repeat of first test

(c) Third test section

Fig. 3 Plots of the results of water injection tests

Analysis of Stable Seepage Conditions

During the injection tests, after seepage began in the test sections and the pumped pressure was increased to a certain level, cracks propagated only slightly, and the observed water pressure and flow rate were relatively stable (Fig. 4). This level of seepage can be defined as the stable seepage and the corresponding maximum stable water pressure is the stable water pressure (P_s). The water pressure test results at this stage can be considered to be a stable seepage condition. Similarly, stable water pressure, seepage pressure difference, and seepage resistance can be used as the basis for evaluating the permeability of the rock mass (Table 3).

As Table 3 shows, the water pressure during stable seepage conditions and seepage resistance both exceed the initial pressure of the seepage water. The seepage pressure difference of the rock mass of the first and second test sections was less than that of the initial water injection test. The observed water pressure exceeded that of the first water injection test, which shows that there were some cracks in the stable seepage phase. The water pressure during this phase is similar in the three test sections, within the range of 8.5–11.0 MPa, with a seepage resistance of ≈3.0 MPa/m. The test results show that the permeability of the rock mass is low and large cracks had not formed. The degree of penetration is still relatively low, and actual seepage can take place under a high water pressure gradient.

Analysis of Permeability Characteristics

The hydraulic conductivity of the test sections in a stable seepage condition can be calculated in accordance with the measured water pressure. If it is assumed that the permeability of the test sections is isotropic and homogeneous, and the water flow during the water injection test is turbulent, not laminar, the total flow rate at any cross section is equal when the flow rate and water pressure are relatively stable (Fig. 5). Therefore, when the flow rate is stable, the hydraulic conductivity of the rock mass can be calculated

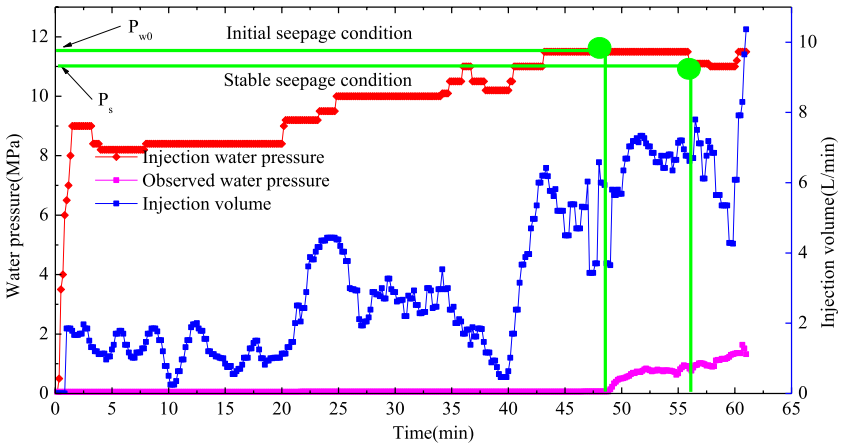

Fig. 4 Schematic diagram of initial point of infiltration and point of steady infiltration

Table 2 Measured water pressure of initial seepage

Test section	Initial seepage water pressure (MPa)	Observed water pressure (MPa)	Seepage pressure difference (MPa)	Seepage resistance (MPa/m)
1st section	8.03	0.06	7.97	2.68
2nd section	11.50	0.32	11.18	3.83
3rd section	7.50	0.30	7.20	2.50

Table 3 Measured water pressure of stable seepage

Test section	Stable seepage water pressure (MPa)	Observed water pressure (MPa)	Seepage pressure difference (MPa)	Seepage resistance (MPa/m)
1st section	8.50	0.09	7.41	2.83
2nd section	11.00	1.20	9.80	3.67
3rd section	9.00	0.53	8.47	3.00

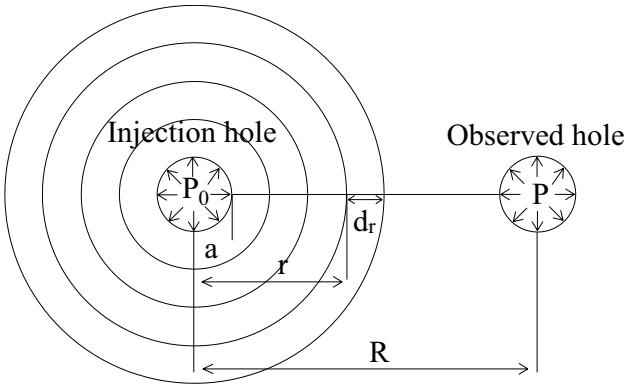

Fig. 5 Analytical diagram of water flow of water injection test

using Eq. (1), in accordance with the relationship between the water injection and observed water pressures (Zhang et al. 2011).

$$k = \frac{Q(\ln R - \ln r)}{2\pi L(H_{P_0} - H_p)} \quad (1)$$

where K is the hydraulic conductivity (cm/s), Q is the injection flow rate (cm^3/s), R is the distance from the injection borehole to the observation borehole (m), r is the diameter of the borehole (m), H_{P_0} and H_P are the water head of positions r and R (cm), P_0 is the injection water pressure (MPa), P is the observed water pressure (MPa), and L is the length of the tested section which is injected with water (cm).

As shown in Fig. 4, the injection water pressure increased quickly from 0 to 9 MPa in less than one minute in the initial water injection test. At the same time, the flow rate increased quickly from 0 to 2 L/min, but the observed water pressure was very low, indicating that the intact rock mass was not conducting water, and originally had a strong seepage resistance. According to homogeneous rock mass destruction mechanism (Fig. 6), with the water injection pressure gradually increasing from 1 to 56 min, there were a lot of small splitting incidents during the high water pressure test. The injection flow rate fluctuated from 3.8 to 7.8 L/min, with each larger flow change corresponding to the fracturing of the rock mass or extension of existing fractures (Jiang et al. 2014). But the observed water pressure stayed low, indicating that the new fractures and fracture extension were small, and did not form good continuous channels during the test. After 56 min, a larger fracture formed, injection water pressure decreased rapidly, the flow rate increased rapidly, and the observed water pressure obviously increased, but the observed water pressure was still much less than the injection water pressure. This shows that only a few fracture channels may have formed. The high water pressure test apparently produced a water diffusion circle, but the channels of seepage were mainly micro-fractures. It can be

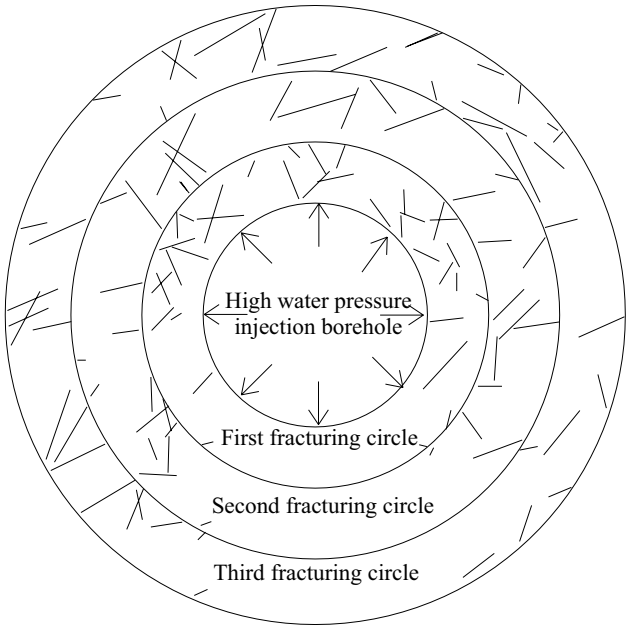

Fig. 6 Sketch of hydraulic fracturing processes of homogeneous rock mass

deduced that the coal seam floor had strong seepage resistance and low seepage during the initial water injection test.

Figure 7 shows the variation in hydraulic conductivity with time when the first water injection test was repeated. The hydraulic conductivity of the repeated test exceeded the water pressure of the first test. The maximum hydraulic conductivity of the two water injection tests (Table 4) was 8.936×10^{-6} cm/s. The hydraulic conductivities shows that the permeability of the intact rock mass of the coal seam floor was low. To increase the accuracy of the test results, we carried out a water injection test on the rock mass of the coal seam floor in another deep mine called the Dongtan coal mine in the Yanzhou coalfield, in which the floor strata is geologically similar to those of the Chengjiao Mine. The hydraulic conductivities are provided in Table 5 (Zhang et al. 2015).

Evaluation of Coal Seam Floor Water Resistance

The safety of mining above a confined aquifer mainly depends on the structure and water-resistance of the coal seam floor. The water inrush coefficient is widely used as a quantitative index to evaluate the risk of water inrush through the seam floor. The determination of the critical water inrush value is key to evaluating the risk of a water inrush. In the latest Provisions on Prevention and Control of Water in Coal Mines (State Administration of Coal Mine Safety 2009), the critical water inrush coefficients of tectonic disturbed and intact floor are based on the statistics of an example of water inrush from a mine floor, so the applicability of the Chengjiao Mine needs

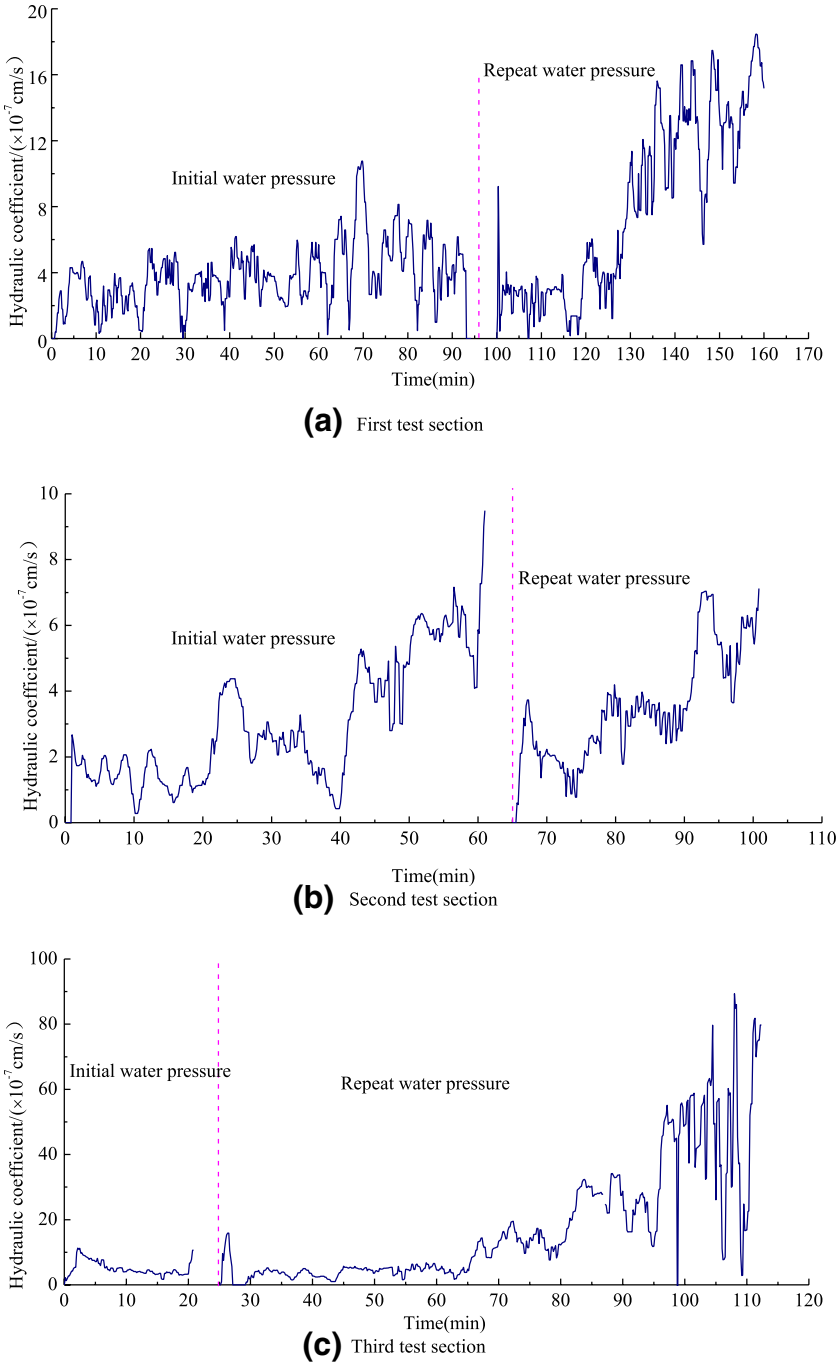

Fig. 7 Variations in plotted permeability with time

Table 4 Maximum hydraulic conductivity values for each test section

Permeability conditions	1st section 1st test	1st section 1st test repeated	2nd section 1st test	2nd section 1st test repeated	3rd section 1st test	3rd section 1st test repeated
Maximum hydraulic conductivity ($\times 10^{-6}$) (cm/s)	1.076	1.846	0.949	0.711	1.130	8.936

Table 5 Maximum hydraulic conductivity for each test section: Dongtan Coal Mine

Permeability conditions	1st section 1st test	1st section Repeat of 1st test	2nd section 1st test	2nd section Repeat of 1st test	3rd section 1st test	3rd section Repeat of 1st test
Maximum hydraulic conductivity ($\times 10^{-6}$) (cm/s)	0.057	0.177	0.064	0.273	0.248	0.145

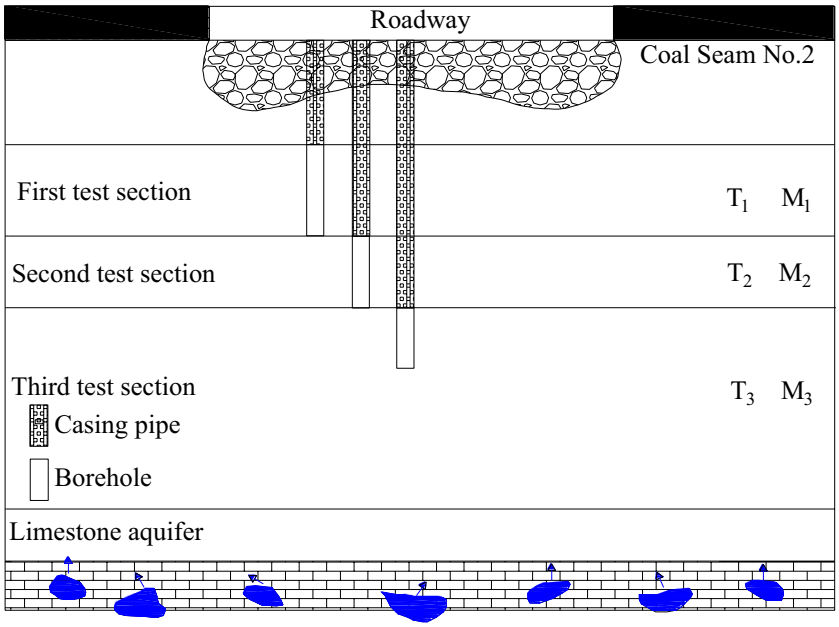

Fig. 8 A general sketch of the floor water inrush

further verification. Therefore, an in-situ water injection test was used, and a large amount of data was measured. As shown in Fig. 8, the limestone is rich in water, so Eq. (2) was used to calculate the water resistance of the overlying strata and to assess the risk of an inrush through the floor.

$$T = \sum_{i=1}^{3} \sigma_i M_i \tag{2}$$

where T is the water-resistance (MPa), σ is the seepage resistance (MPa/m), M is the thickness of the test section (m), and P_0 is the water pressure of limestone aquifer (MPa).

According to Eq. (2), T is the water-resistance of the three test sections and P_0 is the water pressure of the limestone aquifer and the possibility of an inrush from the floor is judged by the relationship between P_0 and T. When $T > P_0$, no water inrush will occur; conversely, if a water inrush occurs, $T < P_0$.

Conclusions

In-situ water injection tests are one of the most reliable ways to determine the permeability of floor strata in deep mines. The analysis and discussion above allow the following conclusions to be drawn.

1. The lowest initial pressure of the seepage water was 7.50 MPa. The observed water pressure of the three test sections was 0.06, 0.32, and 0.30 MPa, respectively. The seepage resistance of the three test sections all exceeded 2.50 MPa/m. Therefore, it can be concluded that the seepage channels are mainly micro-fractures.
2. The water pressure in a stable seepage condition and observed water pressure of the three test sections were 8.50 and 11.00 MPa; 9.00 and 0.09 MPa; and 1.20 and 0.53 MPa, respectively. Compared to the first water

injection test, the water pressure and observed water pressure were higher in a stable seepage condition. This indicates that the produced cracks propagated; however, while stable seepage conditions do not mean structural damage has taken place in the rock mass, continual seepage does indicate partial crushing. According to the measured results, the seepage resistance of the three tested sections was greater than 2.83 MPa/m. In other words, the permeability of the intact rock mass of the coal seam floor is low, and therefore prevents water seepage.

3. The hydraulic conductivity was determined twice for the first water injection tests in the three test sections, in accordance with Eq. (1). The maximum hydraulic conductivity of the first injection test was 1.130×10^{-6} cm/s; however, that of the repeat of the first test was 8.936×10^{-6} cm/s. The maximum hydraulic conductivity in the Dongtan mine is 0.273×10^{-6} cm/s. As a whole, the permeability of rock mass was higher when the first water injections was repeated, and seepage channels formed. Still, the maximum hydraulic conductivity of the three test sections was only 8.936×10^{-6} cm/s. This indicates that the permeability of the intact coal seam floor was low for both first injection tests.
4. The relationship between water resistance and water pressure of the limestone aquifer can be used to assess the risk of a water inrush through the mine floor. If $T < P_0$, then a water inrush can occur, and measures should be taken to prevent an inrush.

Acknowledgements This research was supported by the Fundamental Research Funds for the Central Universities (2015XKMS035) and the Priority Academic Program Development of Jiangsu Higher Education Institutions (PAPD). The authors thank the anonymous reviewers for their helpful comments on the manuscript.

References

Guo WB, Xu FY (2016) Numerical simulation of overburden and surface movements for Wongawilli strip pillar mining. Int J Min Sci Tech 26(1):71–76

Huang Z, Jiang ZQ, Zhu SY, Qian ZW, Cao DT (2014) Characterizing the hydraulic conductivity of rock formations between deep coal and aquifers using injection tests. Int J Rock Mech Min Sci 71:12–18

Huang Z, Jiang ZQ, Fu JJ, Cao DT (2015) Experimental measurement on the hydraulic conductivity of deep low-permeability rock. Arab J Geo Sci 8:5389–5390

ISBN 978-7-5020-3586-0 State Administration of Work Safety (2009) Provisions on prevention and control of water in coal mines [M]. China Coal Industry Press, Beijing, pp 62–63

Jiang ZM, Fu S, Li SG, Hu DK, Feng SR (2014) High pressure permeability test on hydraulic tunnel with steep obliquity faults under high pressure. Chin J Rock Mech Eng 26 (11):2318–2323

Jin J, Cao P, Chen Y, Pu CZ, Mao DW, Fan X (2017) Influence of single flaw on the failure process and energy mechanics of rock-like material. Comput Geotechol 86:150–162

Kitagawa Y, Kano Y (2016) Changes in permeability of the Nojima fault damage zone inferred from repeated water injection experiments. Earth Planets Sp 68:185–193

Li P, Qian H (2013) Global curve-fitting for determining the hydrogeological parameters of leaky confined aquifers by transient flow pumping test. Arab J Geo Sci 6 (8):2745–2753

Li P, Qian H, Wu J, Liu H, Lyu X, Zhang H (2014a) Determining the optimal pumping duration of transient pumping tests for estimating hydraulic properties of leaky aquifers using global curve-fitting method: a simulation approach. Environ Earth Sci 71(1):293–299

Li P, Qian H, Wu J (2014b) Comparison of three methods of hydrogeological parameter determination in leaky aquifers using transient flow pumping tests. Hydrol Process 28(4):2293–2301

Liu RX, Cao DT, Hu DX (2016) A study of the impermeability of the lower coal seam floor rocks at the Yanzhou coalfield based on in-situ test. Hydrogeol Eng Geol 43(1):106–110

Pfunt H, Houben G, Himmelsbach T (2016) Numerical modeling of fracking fluid migration through fault zones and fractures in the North German Basin. Hydrogeol J 24:1343–1358

Xu JP, Zhang FC, Gui H, Zhang TJ (2012) Characteristics and experimental study of water conduction caused by fault activation due to mining. Int J Min Sci Tech 41(3):415–419

Zhang XM, Jiang ZM, Feng SR, Chen SH (2011) Study on the determination of permeability coefficient of fractured rock mass under high pressure test condition. J Hydroelectr Eng 30(1):156–159

Zhang WJ, Zhang XW, Zhang D (2015) Experiment of reduction infiltration ability of rock formation under the coal seam floor at Dongtan Coal Mine. Coal Mine Modern 3:82–85

Zheng D, Frost JD, Huang RQ, Liu FZ (2015) Failure process and modes of rockfall induced by underground mining: a case study of Kaiyang phosphorite mine rockfalls. Eng Geol 197:145–157

Zhu SY, Lu LL, Wu Y, Zhang TT (2017) Comprehensive study on deformation and failure characteristics of the mining-impacted deep double-longwall working faces floor. J Geophys Eng 14(3):641–653